Rht18 Semidwarfism in Wheat Is Due to Increased *GA 2-oxidaseA9* Expression and Reduced GA Content[1][OPEN]

Brett A. Ford,[a] Eloise Foo,[b] Robert Sharwood,[c] Miroslava Karafiatova,[d] Jan Vrána,[d] Colleen MacMillan,[a] David S. Nichols,[e] Burkhard Steuernagel,[f] Cristobal Uauy,[f] Jaroslav Doležel,[d] Peter M. Chandler,[a] and Wolfgang Spielmeyer[a,2]

[a]CSIRO Agriculture and Food, Canberra, ACT 2601, Australia
[b]The School of Natural Sciences, University of Tasmania, Hobart, Tasmania 7001, Australia
[c]Research School of Biology, The Australian National University, Canberra, ACT 0200, Australia
[d]Institute of Experimental Botany, Centre of the Region Haná for Biotechnological and Agricultural Research, CZ-78371 Olomouc, Czech Republic
[e]Central Science Laboratories, University of Tasmania, Hobart, Tasmania 7001, Australia
[f]John Innes Centre, Norwich NR4 7UH, United Kingdom

ORCID IDs: 0000-0002-7467-0950 (B.A.F.); 0000-0002-9751-8433 (E.F.); 0000-0003-4993-3816 (R.S.); 0000-0001-6171-8516 (J.V.); 0000-0003-3594-5373 (C.M.); 0000-0002-8066-3132 (D.S.N.); 0000-0002-8284-7728 (B.S.); 0000-0002-6263-0492 (J.D.); 0000-0003-3840-605X (P.M.C.); 0000-0002-5115-7820 (W.S.).

Semidwarfing genes have improved crop yield by reducing height, improving lodging resistance, and allowing plants to allocate more assimilates to grain growth. In wheat (*Triticum aestivum*), the *Rht18* semidwarfing gene was identified and deployed in durum wheat before it was transferred into bread wheat, where it was shown to have agronomic potential. *Rht18*, a dominant and gibberellin (GA) responsive mutant, is genetically and functionally distinct from the widely used GA-insensitive semidwarfing genes *Rht-B1b* and *Rht-D1b*. In this study, the *Rht18* gene was identified by mutagenizing the semidwarf durum cultivar Icaro (*Rht18*) and generating mutants with a range of tall phenotypes. Isolating and sequencing chromosome 6A of these "overgrowth" mutants showed that they contained independent mutations in the coding region of *GA2oxA9*. *GA2oxA9* is predicted to encode a GA 2-oxidase that metabolizes GA biosynthetic intermediates into inactive products, effectively reducing the amount of bioactive GA (GA_1). Functional analysis of the GA2oxA9 protein demonstrated that GA2oxA9 converts the intermediate GA_{12} to the inactive metabolite GA_{110}. Furthermore, *Rht18* showed higher expression of *GA2oxA9* and lower GA content compared with its tall parent. These data indicate that the increased expression of *GA2oxA9* in *Rht18* results in a reduction of both bioactive GA content and plant height. This study describes a height-reducing mechanism that can generate new genetic diversity for semidwarfism in wheat by combining increased expression with mutations of specific amino acid residues in *GA2oxA9*.

Gibberellins (GAs) are a class of plant hormones involved in many aspects of growth and development, including seed germination, leaf growth, floral induction, and stem elongation (Yamaguchi, 2008). The regulation of plant height, either by lowering the bioactive GA content or by inhibiting GA signaling, formed the basis of the Green Revolution that was associated with major yield increases in wheat (*Triticum aestivum*) and rice (*Oryza sativa*; Hedden, 2003). The wheat semidwarfing genes *Rht-B1b* and *Rht-D1b* encode DELLA proteins that lack a functional DELLA domain, preventing normal GA signaling and resulting in reduced responsiveness to GA and reduced elongation (Peng et al., 1999). The major semidwarfing gene *sd-1* in rice encodes a nonfunctional GA 20-oxidase, a key enzyme in the GA biosynthetic pathway, and causes a lower content of bioactive GA (Sasaki et al., 2002; Spielmeyer et al., 2002). Mutations in GA 20- and GA 3-oxidase biosynthetic genes that reduce plant height have also been identified in other crop species, including maize (*Zea mays*; *dwarf1*) and barley (*Hordeum vulgare*; *sdw1/denso*; Spray et al., 1996; Jia et al., 2015). The GA metabolic enzymes are encoded by multiple genes, often with distinct tissue and developmental specific expression patterns (Pearce et al., 2015). Mutations in stem-expressed GA 20-oxidase, such as in the rice *sd-1* mutant, reduce

[1] M.K., J.V., and J.D. were supported by the Czech Science Foundation (award P501-12-G090) and by the Ministry of Education, Youth, and Sports of the Czech Republic (award LO1204 from the National Program of Sustainability I).

[2] Address correspondence to wolfgang.spielmeyer@csiro.au.

The author responsible for distribution of materials integral to the findings presented in this article in accordance with the policy described in the Instructions for Authors (www.plantphysiol.org) is: Wolfgang Spielmeyer (wolfgang.spielmeyer@csiro.au).

B.A.F., E.F., R.S., and C.M. designed/performed research and analyzed data; M.K., J.V., D.S.N., B.S., C.U., and J.D. contributed analytical skills and/or computational tools; B.A.F., P.M.C., and W.S. conceived experiments and wrote the article.

[OPEN] Articles can be viewed without a subscription.

www.plantphysiol.org/cgi/doi/10.1104/pp.18.00023

plant height without affecting other important GA-dependent processes, such as reproductive development (Spielmeyer et al., 2002). However, unlike the DELLA GA signaling mutants, GA biosynthetic mutants are responsive to the application of GA.

GA biosynthesis in cereals proceeds through a common intermediate GA_{12} that is hydroxylated at C-13 to form GA_{53} before being converted to bioactive GA_1 in a multistep process catalyzed by dioxygenase enzymes (Yamaguchi, 2008; Hedden and Thomas, 2012). The content of GA_1 depends on its rate of synthesis and on the rate at which it is inactivated by 2-oxidation. Different GA 2-oxidase isoforms metabolize GA_1 and its immediate precursor GA_{20} to the inactive GA_8 and GA_{29}, respectively (C_{19} isoforms), or convert the earlier GA biosynthetic intermediates GA_{12} and GA_{53} to the inactive GA_{110} and GA_{97}, respectively (C_{20} isoforms; Sakamoto et al., 2003; Schomburg et al., 2003). Metabolism of biosynthetic intermediates to these inactive products reduces flux through the biosynthetic pathway, leading to a lower GA_1 content and reduced growth (Schomburg et al., 2003; Lo et al., 2008).

A new strategy for reducing height and achieving semidwarf phenotypes has been to overexpress GA 2-oxidase transgenes in a range of species (Busov et al., 2003; Elias et al., 2012; Wuddineh et al., 2015). In wheat, ectopic expression of the bean (*Phaseolus coccineus*) *PcGA2ox1* gene decreased GA content and strongly reduced plant height, but also had pleiotropic effects on growth habit, tillering, and ear size (Appleford et al., 2007). In rice, overexpression of the C_{19} *OsGA2ox1* gene also resulted in severe height reduction, whereas expression of the same transgene using the promoter of a native GA biosynthesis gene yielded plants with semidwarf phenotypes and fewer undesirable characteristics (Sakamoto et al., 2001, 2003). Overexpressing the C_{20} *OsGA2ox6* or *OsGA2ox9* genes in rice resulted in moderate height reductions without affecting time to anthesis or grain production (Lo et al., 2008; Huang et al., 2010). Taken together, these studies demonstrate the agronomic potential of overexpressing GA 2-oxidase transgenes to achieve semidwarf lines with varying degrees of height reduction.

Rht18 is a dominant, semidwarfing gene that was identified following fast neutron mutagenesis of the tall durum wheat variety Anhinga and released as the commercial semidwarf durum cultivar Icaro (Konzak, 1988). *Rht18* has also been introgressed into hexaploid bread wheat, and initial field studies have demonstrated its agronomic potential (Yang et al., 2015; Tang, 2015). In a recent mapping study of two durum RIL (recombinant inbred line) populations, *Rht18* was mapped within an interval of 1.8 centimorgan (cM) on chromosome 6A that contained a GA 2-oxidase gene, *GA2oxA9* (Vikhe et al., 2017). An association mapping study of hexaploid winter wheats identified a major quantitative trait locus for reduced height on chromosome 6A that overlapped with the *Rht18* region and included *GA2oxA9* (Würschum et al., 2017). *Rht18* is GA responsive, as coleoptile length and seedling leaf elongation rates both increased in *Rht18* lines following GA application (Ellis et al., 2004; Vikhe et al., 2017). Given its GA responsiveness and its distinct location from *Rht-B1* and *Rht-D1* (chromosome group 4), *Rht18* represents a semidwarfing gene in wheat that is unrelated to mutant DELLA genes.

In this study, we identified the *Rht18* gene by mutagenizing the semidwarf line Icaro with sodium azide and screening for overgrowth mutations that suppressed dwarfism and produced tall lines. Thirteen such mutants contained independent mutations in the coding region or splice sites of *GA2oxA9*. The transcript levels of *GA2oxA9* were higher, and the GA_1 content lower in semidwarf Icaro compared with its tall parent Anhinga. We also found that the *GA2oxA9* gene encodes a functional enzyme that metabolizes a C_{20} GA precursor (GA_{12}) and that enzyme activity was greatly reduced in one of the overgrowth mutants. The data indicate that the *Rht18* phenotype is caused by increased expression of *GA2oxA9*, resulting in a lower content of bioactive GA. This study highlights how an allelic variant in a GA 2-oxidase gene can regulate growth in a manner that previously has only been observed in transgenic plants.

RESULTS

Rht18 Maps to the Centromeric Region of Chromosome 6A

The *Rht18* semidwarfing gene was previously mapped to chromosome 6A in a region flanked by the single-nucleotide polymorphism (SNP)-based markers *IWA3230* and *IWB62878* in durum wheat (Fig. 1; Tang, 2015). In this study, the flanking markers were used to screen an F2 population derived from a cross between Icaro (semidwarf) and Langdon (tall) durum wheat cultivars to define a genetic interval of approximately 1.5 cM, which contained *Rht18*. *IWA3230* was located at 106 Mb on the short arm and *IWB62878* at 450 Mb on the long arm of chromosome 6A, spanning a centromeric region of approximately 344 Mb on the Chinese Spring wheat genome sequence (Fig. 1). The unfavorable relationship of genetic to physical distance in this region (1 cM/230 Mb) precluded a map-based cloning approach to characterize the *Rht18* locus.

Identification of *Rht18* Overgrowth Mutants in Tetraploid and Hexaploid Wheat

Rht18 behaves as a dominant gene in durum wheat (Tang, 2015) and is a presumed gain-of-function mutant. We predicted that sodium azide induced mutations in the *Rht18* gene would result in loss-of-function (tall) overgrowth derivatives, similar to the strategy recently used to identify second site mutations within the severe DELLA dwarfing allele *Rht-B1c* (Chandler and Harding, 2013). Chromosome 6A could then be sequenced from a set of multiple, independent, allelic mutants and analyzed using recently developed bioinformatics tools to define the gene responsible for the dwarfing phenotype (Sánchez-Martín et al., 2016).

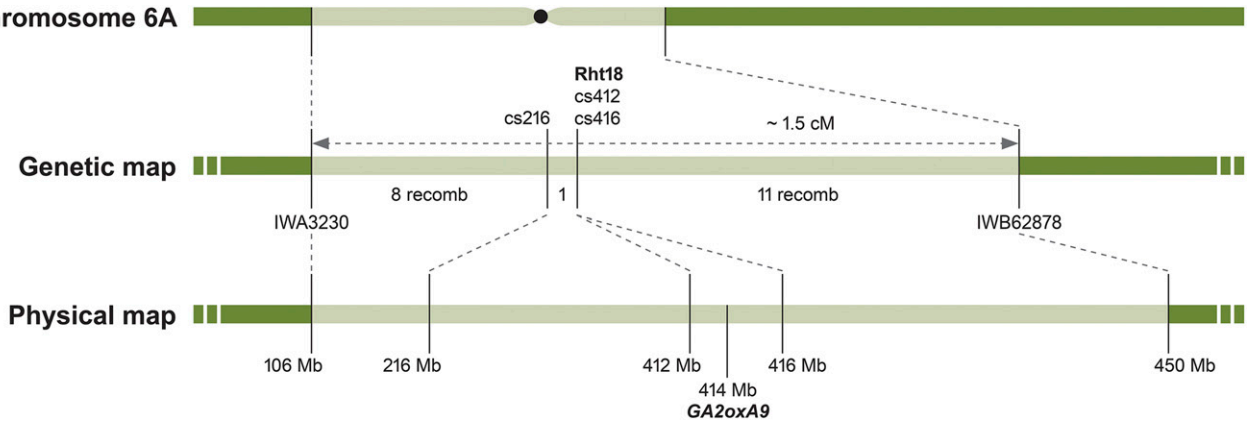

Figure 1. Genetic and physical mapping of *Rht18* region on chromosome 6A. Genetic map developed from Icaro x Langdon F2:F3 mapping population. Markers were mapped to the IWGSC Ref Seq v1.0 wheat genome assembly to determine their physical locations.

Icaro was mutagenized with sodium azide and a bulk M2 population was screened for height in the field. Putative overgrowth mutants were then selected and progeny tested in the glasshouse. Fourteen mutants (ranging in height from 73–121 cm) were confirmed to be taller than Icaro (59 cm) and closer in height to the tall parent Anhinga (94 cm; Fig. 2). Five overgrowth mutants, M12, M17, M22, M24, and M54, which were most likely to represent independent events based on the structure of the M2 population, were selected for further study. Overgrowth mutants were also identified in a hexaploid bread wheat background by screening a sodium azide M2 population of Halberd-*Rht18* for height in the field. Eighty plants judged to be taller than their semidwarf parent were selected, and 30 were subsequently confirmed by progeny testing in the glasshouse. The mean height of the Halberd-*Rht18* overgrowth mutants ranged between 86 and 116 cm, which was taller than the Halberd-*Rht18* parent (61 cm) and closer to the tall Halberd isogenic line (97 cm; Fig. 2).

Mutations in the *GA2oxA9* Gene Are Responsible for the Overgrowth Phenotype

To test the hypothesis that overgrowth mutants carried loss-of-function mutations in *Rht18*, three durum overgrowth mutants (M12, M24, and M54) were

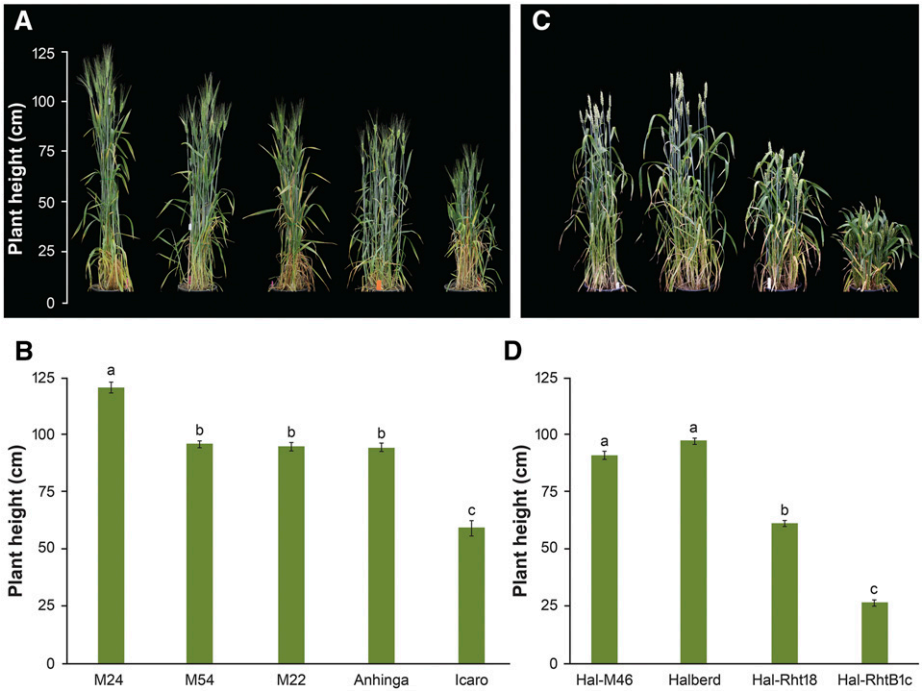

Figure 2. Plant height is increased in *Rht18* overgrowth mutants in tetraploid (A and B) and hexaploid (C and D) wheat. Plant height was measured at maturity and data presented as mean values ± SE (n = 12 for each line). Different letters indicate significant differences in plant height of tetraploid (B) and hexaploid (D) wheats (ANOVA, $P < 0.05$).

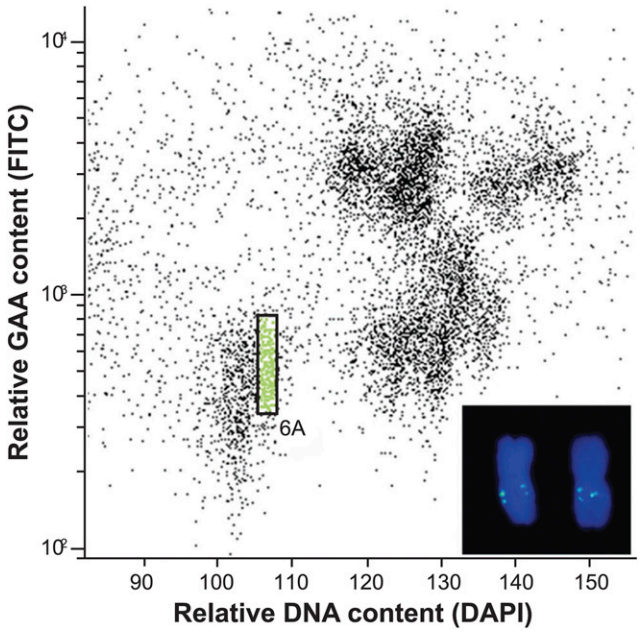

Figure 3. Biparametric flow karyotype of *Triticum durum* cv Icaro. The population of target chromosome 6A is highlighted in green. Inset: Images of two flow-sorted chromosomes 6A. The chromosome was identified using fluorescence in situ hybridization with a probe for GAA microsatellite (yellow-green). Chromosome were counterstained with 4′,6-diamidino-2-phenylindole (DAPI; blue).

intercrossed and outcrossed to Icaro and Anhinga, generating F2 populations for height measurement. Genetic analysis showed that the overgrowth mutations were most likely allelic and either tightly linked to, or within, the *Rht18* gene (see "Materials and Methods"). We hypothesized that overgrowth lines would carry mutations in the *Rht18* gene. We therefore isolated and sequenced chromosome 6A from mutants and Icaro to identify mutations that may be responsible for the overgrowth phenotype. Chromosome 6A was isolated by flow cytometry sorting from Icaro, Anhinga, and the five durum overgrowth mutants, M12, M17, M22, M24, and M54 (Fig. 3). DNA prepared from isolated chromosomes was sequenced at greater than 80× coverage (Fig. 4). Illumina sequence reads from Icaro were assembled de novo, producing an assembly with a total length of 444 Mb (~70% of the total length of 6A) that was predicted to cover most of the genic regions. Raw reads from the overgrowth mutants and Icaro were then mapped to the Icaro assembly and single-nucleotide variants (SNVs) identified (Fig. 4). Contigs that contained at least one independent SNV in each of the five overgrowth mutants were identified; there was only a single contig, from a total of >120,000, which contained five independent SNVs, one in each mutant (Fig. 4; Supplemental Fig. S1). This contig (contig_22631_1) contained a single predicted open reading frame (ORF) that encoded a GA 2-oxidase gene (*GA2oxA9*; Fig. 4). The D subgenome homeolog *GA2oxD9* has been demonstrated to encode an enzyme that metabolizes GA biosynthetic intermediates, potentially lowering the content of bioactive GAs. Thus, *GA2oxA9* was presumed to have a similar function (Pearce et al., 2015).

Nucleotide sequences of the predicted *GA2oxA9* ORF from the five mutants were translated and compared with Icaro and other wheat and rice GA 2-oxidases (Supplemental Fig. S2). All mutations occurred within the predicted coding region of *GA2oxA9*; four mutations involved changes in conserved amino acids, M12 (S295F), M17 (G337R), M22 (G243D), and M54 (G81D), whereas in the fifth mutant, M24 (W252*) a premature termination codon was introduced that was predicted to result in a nonfunctional protein (Fig. 4; Supplemental Fig. S2). Based on these results in durum, we sequenced the *GA2oxA9* gene from Halberd-*Rht18* and eight of the Halberd-*Rht18* overgrowth mutants. Five mutants contained SNVs in the predicted coding region of *GA2oxA9*, resulting in changes in a conserved amino acid, Hal-M13 (S274N), Hal-M26 (T321I), Hal-M30 (T234I), Hal-M46 (R208Q), and Hal-M47 (E64K). One introduced a premature termination codon, Hal-M75 (W80*), and the remaining two mutants Hal-M1 and Hal-M10 contained a SNV that was predicted to change a spliceosome recognition site (Fig. 4; Supplemental Figs. S3 and S4). These data indicate that 13 independent mutations in the *GA2oxA9* gene, in both tetraploid and hexaploid overgrowth lines, are responsible for their enhanced growth through either a loss or reduction in GA2oxA9 protein amount or activity.

Rht18 Semidwarfism Is Associated with Increased Expression of *GA2oxA9*

In the Icaro x Langdon mapping population, SNP-based markers cs_412 and cs_416 that flank *GA2oxA9* in the Chinese Spring physical map cosegregated with *Rht18*. This was consistent with the possibility that *GA2oxA9* is also responsible for the semidwarf phenotype of *Rht18* (Fig. 1). However, the nucleotide sequences of the predicted ORF of *GA2oxA9* were identical in Icaro and Anhinga. We therefore hypothesized that increased gene expression of *GA2oxA9* in Icaro relative to Anhinga could result in a lower GA_1 content and reduced height. This idea was supported by previous studies that have shown that increased expression of closely related GA 2-oxidase genes in wheat, rice, poplar (*Populus tremula* × *Populus alba*) and Arabidopsis (*Arabidopsis thaliana*) result in dwarf phenotypes (Busov et al., 2003; Schomburg et al., 2003; Appleford et al., 2007; Lo et al., 2008).

GA2oxA9 expression was assayed by quantitative, real-time reverse transcriptase PCR (qPCR) in elongating peduncles, as most of the height reduction in Icaro was due to reduced peduncle length. Expression of *GA2oxA9* was ~4-fold higher in the Icaro and the M24 overgrowth mutant compared to the tall parent

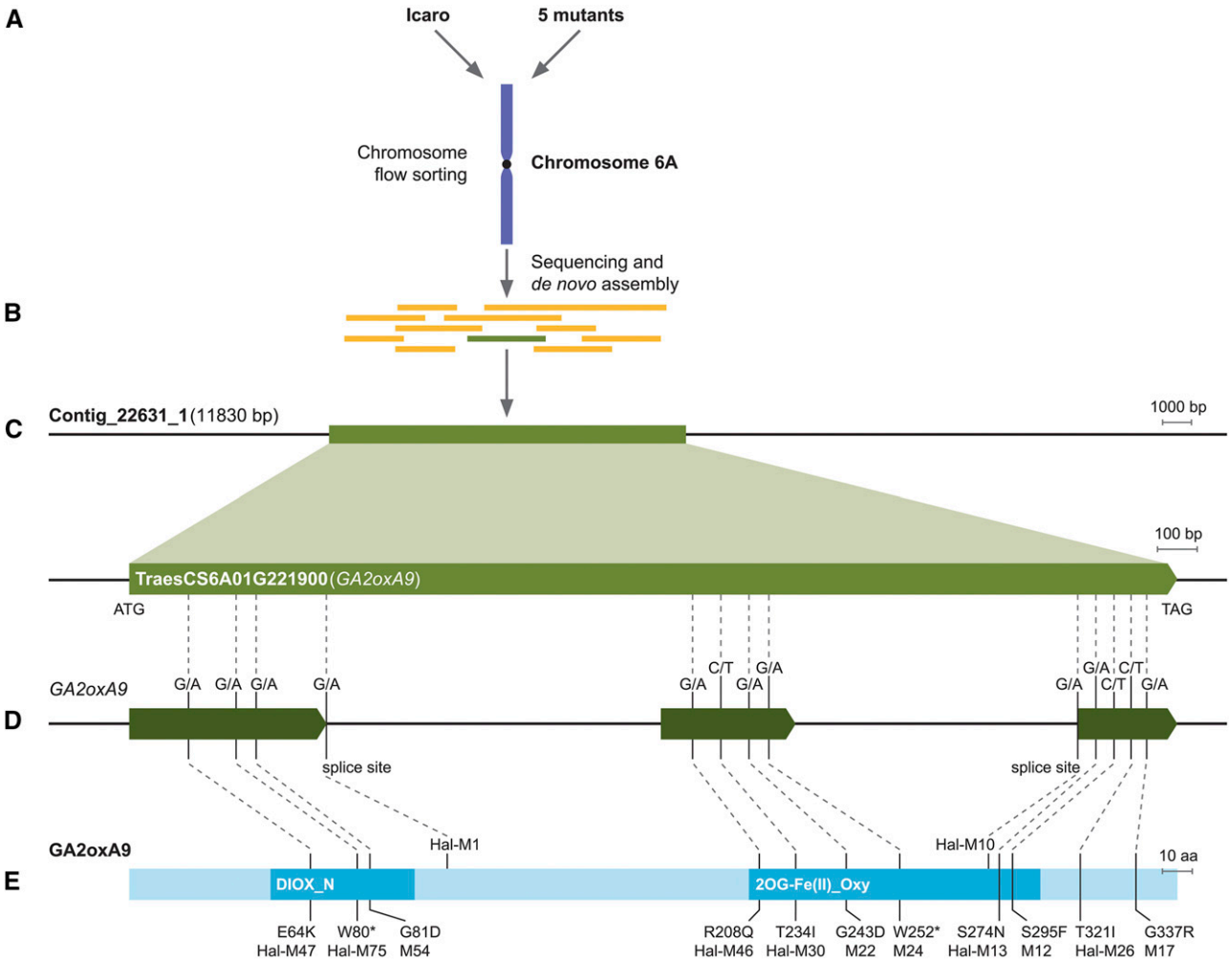

Figure 4. Identification of *GA2oxA9* as a candidate gene for *Rht18*. A, Chromosome 6A from Icaro and overgrowth mutants isolated and Illumina-sequenced at greater than 80× coverage. B, Icaro Illumina reads de novo assembled and sequence of the overgrowth mutants mapped back to the assembly. C, Contig (22631_1) was identified which contained gene TraesCS6A01G221900 (*GA2oxA9*). D, Gene model of *GA2oxA9* showing three exons and five independent mutations (G/A or C/T transitions) in durum Icaro background. Additional mutations were found in eight Halberd overgrowth mutants (Hal-M47, Hal-M75, Hal-M13, Hal-M46, Hal-M30, Hal-M10, Hal-M1, and Hal-M26). E, Predicted amino acid sequence of GA2oxA9 protein showing single amino acid substitutions in durum and hexaploid wheat mutants except in M24 and Hal-M75 where mutations resulted in early termination codons and Hal-M1 and Hal-M10 where mutations resulted changing spliceosome recognition site. Predicted functional domains include nonhaem dioxygenase (DIOX_N) domain and 2-oxoglutarate and Fe(II)-dependent oxygenase [2OGFe(II)_Oxy] domain.

Anhinga (Fig. 5A). *GA2oxA9* expression was also determined in fixed short and tall segregants from the Icaro x Langdon mapping population. The expression level of *GA2oxA9* was higher in Icaro and the fixed short progeny compared to the Langdon and fixed tall progeny (Fig. 5A). Previously, another semidwarf mutant Castelporziano (*Rht14*) was identified following the treatment of the tall durum wheat Capelli with fast neutron radiation (Gale et al., 1985). Genetic studies have shown that *Rht14* is probably allelic to *Rht18* (Haque et al., 2011; Tang, 2015). The nucleotide sequences of the predicted *GA2oxA9* ORF from Castelporziano and Capelli were identical to Icaro and Anhinga. Like Icaro, *GA2oxA9* expression was also increased in Castelporziano compared to its tall parent Capelli (Fig. 5A). As both Icaro and Castelporziano are tetraploid wheats, the expression of the homeologous gene on the B genome (*GA2oxB9*) was also assayed in peduncle tissue. In Icaro, M24, Anhinga, Castelporziano, and Capelli, *GA2oxB9* expression was below the limit of detection by qPCR.

Expression of *GA2oxA9* was also assayed in the Halberd bread wheat (hexaploid) background. Similar to the results seen in the tetraploid lines, expression of *GA2oxA9* was increased in Halberd-*Rht18* and the Halberd-*Rht18* overgrowth mutants Hal-M10 and

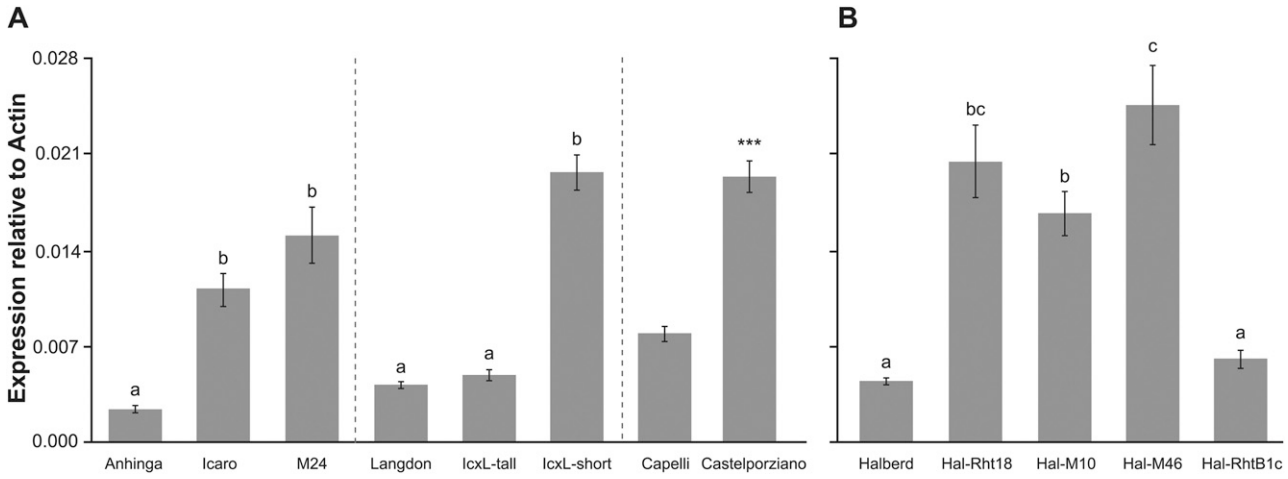

Figure 5. *GA2oxA9* expression is increased in *Rht18* and *Rht14* wheat isolines. *GA2oxA9* expression relative to actin in elongating peduncle tissue from tetraploid (A) and hexaploid (B) wheat. Data are mean values of four biological replicates ± SE. Different letters indicate significant differences between Anhinga, Icaro (*Rht18*), and M24, between Langdon, fixed tall, and fixed short segregants from Icaro x Langdon mapping population, and between Halberd-*Rht18* isolines (ANOVA, $P < 0.05$). Significant differences between Castelporziano (*Rht14*) and Capelli are indicated by asterisks (Student's *t* test,***$P < 0.001$).

Hal-M46 compared to Halberd (Fig. 5B). The fold change in expression was similar in magnitude across tetraploid and hexaploid isolines. *GA2oxA9* expression was also determined in a severe Halberd dwarf carrying the mutant DELLA *Rht-B1c* allele (Fig. 2). The expression of *GA2oxA9* was similar in Halberd-*Rht-B1c* compared to Halberd (Fig. 5B), indicating that the increased expression of *GA2oxA9* in Halberd-*Rht18* is not simply a consequence of short plant stature.

Expression of *GA2oxA9* was also determined in elongating first leaves, where the rate of leaf elongation was lower in Icaro compared with Anhinga and M24 (Supplemental Fig. S5). Similar to the results observed in peduncle tissue, expression of *GA2oxA9* was increased in Icaro, M24, and Castelporziano compared to the tall parents Anhinga and Capelli (Supplemental Fig. S5). Taken together, these data show a consistent increase in *GA2oxA9* expression in elongating peduncle and leaf tissue of semidwarf lines relative to tall parents in both tetraploid and hexaploid wheat.

Rht18 Semidwarfism Is Associated with a Lower Content of Bioactive GA

The increase in *GA2oxA9* expression observed in *Rht18* and *Rht14* relative to tall lines is consistent with the hypothesis that increased expression of this gene leads to semidwarfism associated with a lower content of bioactive GA. GA contents were determined in elongating peduncle tissue of both sets of tall and semidwarf isogenic lines (Fig. 6). The content of bioactive GA_1 was substantially reduced in the semidwarf lines Icaro and Castelporziano compared to tall lines Anhinga and Capelli (Fig. 6D). The levels of GA precursors were also lower in Castelporziano (GA_{53}, GA_{19}, and GA_{20}), as was the GA_1 catabolite GA_8 in both Icaro and Castelporziano, suggesting that the lower content of GA_1 was the result of reduced flux through the GA biosynthetic pathway (Fig. 6). The content of several endogenous GAs in the M24 overgrowth mutant was greater than in Icaro and similar to the tall isoline Anhinga, consistent with a nonfunctional GA2oxA9 protein resulting from a newly introduced termination codon (Figs. 4 and 6).

GA2oxA9 Encodes a Functional GA 2-Oxidase That Inactivates GA_{12}

GA2oxA9 is a member of the C_{20} GA 2-oxidase family, which have been shown to catalyze the conversion of the C_{20} GA biosynthetic intermediates GA_{12} and GA_{53} to inactive GA_{110} and GA_{97}, respectively (Schomburg et al., 2003; Lo et al., 2008). The biochemical function of GA2oxA9 was evaluated by expressing the *GA2oxA9* gene from Icaro and the M24 overgrowth mutant in *Escherichia coli* (see "Materials and Methods"). The GA2oxA9 protein from Icaro converted most of the radiolabeled $[^{14}C_1]GA_{12}$ substrate to $[^{14}C_1]GA_{110}$ within 1 h of incubation (Fig. 6F). In comparison, in a parallel assay with the protein from M24, much less GA_{110} was formed and more of the substrate was retained, indicating that the mutant protein was able to catalyze $[^{14}C_1]GA_{12}$ to $[^{14}C_1]GA_{110}$ but with greatly reduced efficiency compared with Icaro (Fig. 6F). When similar assays were carried out with $[^{14}C_1]GA_1$ and $[^{14}C_1]GA_{20}$, no $[^{14}C_1]GA_8$ or $[^{14}C_1]GA_{29}$ products were detected, respectively (data not shown), indicating the enzyme may be specific for C_{20} 2-oxidation steps. Although the mutation in M24 was predicted to result in a premature termination codon and a nonfunctional protein in

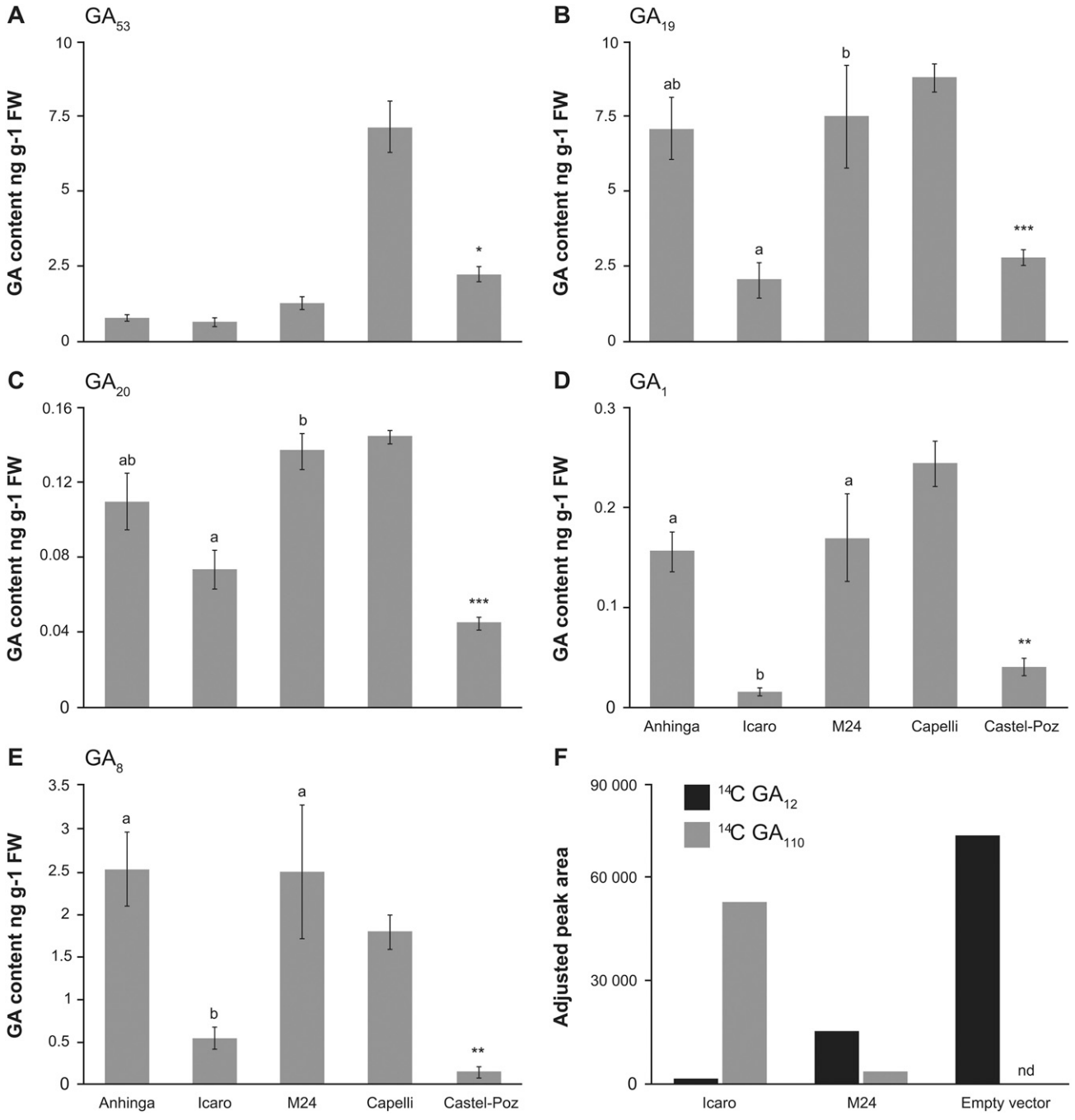

Figure 6. GA content in Icaro (*Rht18*), Castelporziano (*Rht14*), and respective tall isolines and enzyme activity of GA2oxA9 from Icaro (*Rht18*) and tall isoline (M24). A to E, Content of GA precursors GA_{53}, GA_{19}, and GA_{20} (A–C), bioactive GA_1 (D), and inactive catabolite GA_8 (E; ng/g FW) in rapidly elongating peduncle tissue from tetraploid wheat lines. Data are mean values of three biological replicates ± SE. Different letters indicate significant differences between Icaro (*Rht18*), M24, and Anhinga (ANOVA, $P < 0.05$). Significant differences between Castelporziano (*Rht14*) compared to Capelli are indicated by asterisks (Student's *t* test, $*P < 0.05$, $**P < 0.01$, and $***P < 0.001$). F, Adjusted peak areas of ^{14}C-GA_{12} and product ^{14}C-GA_{110} following 1 h incubation of ^{14}C-GA_{12} with cell-free extracts from *E. coli* expressing *GA2oxA9* from *Rht18* (Icaro), tall mutant (M24), and empty vector control monitored by liquid chromatography-tandem mass spectrometry. Extracts from *E. coli* with empty vector control had no detectable (nd) ^{14}C-GA_{110}.

planta, some functional protein must have been expressed in *E. coli* to enable the catalysis of substrate, since no activity was detected in the empty vector control. The result of the functional analysis was consistent with some predicted full-length protein being detected on the SDS-PAGE gel separating protein

extracted from *E. coli* expressing the M24 construct (Supplemental Fig. S6).

GA2oxA9 Promoter and Upstream Sequences Are Highly Conserved in Icaro and Anhinga

To elucidate DNA polymorphisms that could be responsible for the differential expression of *GA2oxA9*, we compared 100 kb of Icaro sequence immediately upstream from the predicted transcription start site of *GA2oxA9* with Anhinga using the Chinese Spring IWGSC RefSeq v1.0 reference genome assembly (https://wheat-urgi.versailles.inra.fr/). The *GA2oxA9* promoter and upstream sequence were highly conserved (Supplemental Fig. S7) with only 13 SNPs detected between Icaro and Anhinga and the closest SNP being 7,314 bp upstream of the transcriptional start site (Supplemental Table S1). The 100-kb sequence of the IWGSC RefSeq 1.0 assembly was identical to the recently released sequence in the *Triticum* 3.1 assembly (Zimin et al., 2017). The sequences of the 3′ untranslated regions of Anhinga and Icaro were also identical, indicating that transcript stability was unlikely to play a role in the differential expression of the gene. As mutations induced by fast neutron radiation are characterized by the introduction of small deletions, we identified all deletions 5 Mb upstream of the predicted transcription start site of *GA2oxA9* in Icaro compared to Anhinga (Supplemental Table S2). Eight deletions ranging in size from 1 to 32 bp were identified, the closest being a 1 bp deletion ~0.8 Mb upstream of *GA2oxA9* (Supplemental Table S2). It is possible that sequence divergence between Anhinga and Chinese Spring prevented the identification of causal deletions in Icaro. Increased expression of *GA2oxA9* is likely to have resulted from the fast neutron mutagenesis, and the results from the fine mapping showed that the causal change must be tightly linked to the *Rht18* locus. Future work will focus on identifying this causal mutation.

DISCUSSION

The *GA2oxA9* gene was identified through a combination of genome complexity reduction, next-generation sequencing, and the application of bioinformatics tools to find causal SNVs in 13 independent mutants. Recent technological and scientific advances in all these areas allow researchers to isolate wheat genes while bypassing lengthy and laborious recombination-based mapping and cloning procedures. In particular, the ability to isolate individual wheat chromosomes in most genetic backgrounds constitutes a paradigm shift in complexity reduction of the wheat genome (Giorgi et al., 2013). A key advantage of whole-chromosome sequencing and analysis using the MutChromSeq protocol compared to other strategies such as RNA-seq or exome capture is that it provides a nonbiased approach to target causal SNVs in protein coding and regulatory sequences alike (Sánchez-Martín et al., 2016). The MutChromSeq approach is particularly useful for target regions close to centromeres, which are difficult to analyze using recombination-based approaches. The mutations in *GA2oxA9* were identified without any prior knowledge of detailed map information of the gene on chromosome 6A.

We propose the following model for *GA2oxA9* regulation of plant height (Fig. 7): In the tall parent Anhinga, the production of GAs proceeds through the intermediates GA_{12}, GA_{53}, GA_{44}, GA_{19}, and GA_{20} to bioactive GA_1 (Hedden and Thomas, 2012). In the semidwarf Icaro, there is increased expression of *GA2oxA9* and enhanced conversion of GA_{12} to GA_{110}, resulting in decreased flux through the biosynthetic pathway and ultimately lower bioactive GA_1 (Fig. 7). This lower content of bioactive GA_1 results in reduced plant height in Icaro (Fig. 7). In the overgrowth mutant M24, the function of the GA2oxA9 protein is impaired and the conversion of GA_{12} to GA_{110} is greatly reduced, allowing normal flux through the GA biosynthetic pathway and thereby restoring normal GA_1 content and plant height (Fig. 7). Thus, a single gene, *GA2oxA9*, is most likely responsible for both the semidwarf *Rht18* and the overgrowth phenotypes in durum and bread wheat.

The mutation in the M24 overgrowth mutant introduced an early termination codon and the line was taller than wild-type Anhinga, indicating that *GA2oxA9* may play a role in the regulation of plant height. However, in our study, we could only detect very low expression of *GA2oxA9* in the expanding peduncle tissue of Anhinga (Fig. 5). *GA2oxA9* was expressed in bread wheat during the early stages of stem elongation (Pearce et al., 2015), indicating that the *GA2oxA9* gene may regulate plant height, but at an earlier time point than that assessed in our study.

An increase in expression of a GA metabolic gene resulted in a lower bioactive GA content and the *Rht18* semidwarf phenotype. This mechanism is distinct from mutant DELLA genes *Rht-B1b* and *Rht-D1b* that disrupt GA signaling in wheat and from height-reducing mechanisms in other crop species (Peng et al., 1999; Sasaki et al., 2002; Spielmeyer et al., 2002). In barley and rice, semidwarfism is also caused by a reduced bioactive GA content, but this is achieved through loss of function mutations in key GA biosynthetic genes (Sasaki et al., 2002; Spielmeyer et al., 2002; Jia et al., 2015). Such loss-of-function mutants have not been isolated in wheat, most likely due to the presence of closely related, functional gene members in the two (durum) or three (bread wheat) subgenomes (Borrill et al., 2015). In contrast, mutations that increase expression of a GA 2-oxidase gene like *Rht18* are dominant gain-of-function mutants that are largely unaffected by gene redundancy in polyploid wheat.

The regulation of plant height by increased expression of GA 2-oxidase has been reported in numerous studies that overexpressed members of this gene family ectopically or by activation-tagged mutants (Sakamoto et al., 2001; Sakai et al., 2003; Appleford et al., 2007; Lo

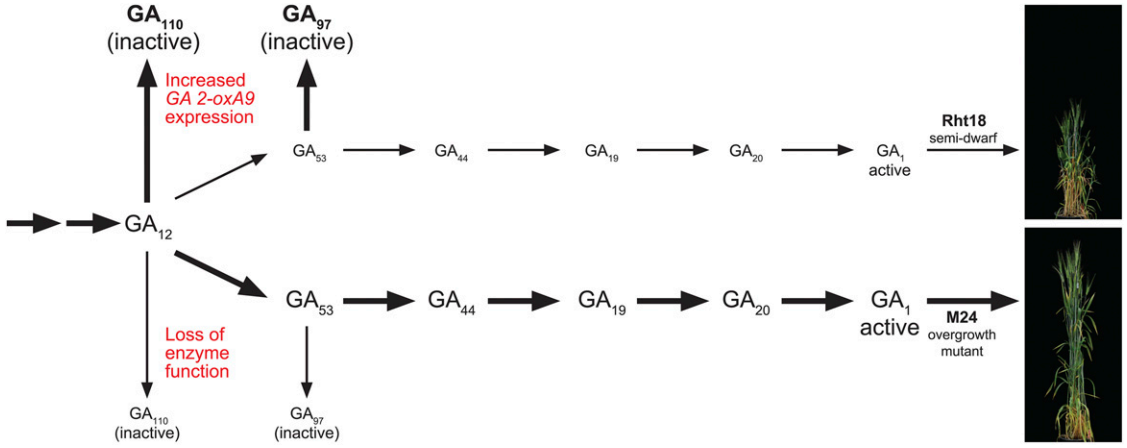

Figure 7. *GA2oxA9* is responsible for semidwarf and overgrowth phenotypes. Increased expression of *GA2oxA9* stimulates conversion of GA_{12} and GA_{53} to inactive GA_{110} and GA_{97}, respectively. This reduces flux in the GA biosynthetic pathway, resulting in lower contents of bioactive GA_1 and semidwarfism. Mutations in *GA2oxA9* cause loss of protein function and impair the conversion of GA_{12} and GA_{53} to inactive GA_{110} and GA_{97}. This restores flux through the GA biosynthetic pathway, increasing GA_1 content and restoring plant height.

et al., 2008). However, constitutive expression of GA 2-oxidases often results in severe height reduction and reduced fertility (Sakamoto et al., 2001; Sakai et al., 2003; Appleford et al., 2007; Lo et al., 2008). Here, we report nontransgenic wheat mutants with changes in both expression and coding sequence in a GA 2-oxidase gene that controls plant height. A combination of increased gene expression and mutations in conserved amino acid residues generates a range of semidwarf heights in durum and hexaploid wheat. This strategy was used in transgenic rice to generate height variants with improved agronomic performance (Lo et al., 2017). Constitutive expression of mutant C_{20} *OsGA2ox6* isoforms carrying single amino acid changes generated transgenic rice lines with increased yield potential and stress tolerance compared to lines that express the wild-type C_{20} *OsGA2ox6* gene under the control of the endogenous promoter (Lo et al., 2017). The increased expression of the C_{20} *GA2oxA9* in *Rht18* has also generated semidwarfs with agronomic potential and provides a nontransgenic approach to further increase genetic diversity by combining with mutations in conserved amino acid residues (Yang et al., 2015). In this study, we have generated more than 30 overgrowth mutants in hexaploid and tetraploid wheat that may prove to be a valuable source of new semidwarfing alleles.

Rht14 and *Rht24* Are likely Alleles of *Rht18*

Rht14 and *Rht18* were previously reported to be linked to the same simple sequence repeat marker on chromosome 6A and the analysis of progeny from intercrosses showed that these genes were likely to be alleles (Haque et al., 2011; Tang, 2015). In Castelporziano (*Rht14*), *GA2oxA9* expression was increased and GA content decreased relative to a tall isogenic line mirroring the changes observed between *Rht18* isogenic lines (Figs. 5 and 6). These data support the hypothesis that *Rht14* and *Rht18* are allelic and that the semidwarf phenotype of *Rht14* is the result of increased expression of *GA2oxA9*. The *Rht14* and *Rht18* semidwarfs were identified by separate groups in fast neutron mutagenized populations of two different tall durum genetic backgrounds. The predicted ORFs of *GA2oxA9* were identical between mutants and wild types, so changes in gene expression most probably were responsible for the mutant phenotype. What is the molecular basis that led to changes in gene expression in these mutants? These changes may have arisen because of either mutagen treatment or by spontaneous events. Comparison of sequences upstream of the predicted transcription start sites between mutant and the wild type did not reveal any characteristic small deletions that are typical following treatment with fast neutron radiation (Supplemental Table S1; Koornneef et al., 1982). Changes in chromatin structure were recently linked to the regulation of GA 2-oxidase gene in Arabidopsis root meristems (Li et al., 2017b). Future work will investigate the molecular basis of increased expression of *GA2oxA9* in Icaro and Castelporziano. Another major quantitative trait locus for reduced height (*Rht24*) was recently reported in an association mapping study of European winter wheats (Würschum et al., 2017). The map location of *Rht24* overlapped the *Rht18* region on chromosome 6A that included *GA2oxA9*. Natural variation in gene expression and/or allelic diversity in the ORF of *GA2oxA9* may be responsible for reducing height in winter wheat cultivars, suggesting that this locus is already playing a role in wheat improvement.

CONCLUSION

Characterizing *Rht18* has provided insight into a new height reducing mechanism for wheat by linking an

induced mutant to an increase in expression of a GA 2-oxidase gene. We anticipate that this discovery will generate additional variation for height by combining increased expression with specific amino acid changes in GA 2-oxidase to develop a range of semidwarfs independent of mutant DELLA genes in one of the most important food crops.

MATERIALS AND METHODS

Plant Material and Growth Conditions

The tetraploid wheat (*Triticum aestivum*) Icaro (*Rht18*) and Castelporziano (*Rht14*) were derived from independent fast neutron treated populations (Gale et al., 1985; Konzak, 1988). Tetraploid wheats and the hexaploid wheat Halberd were obtained from the Australian Winter Cereals Collection. Halberd-*Rht18* and Halberd-*Rht-B1c* are BC_4F_4 fixed near isogenic lines that were developed at CSIRO. Plants used for assessment of plant height, *GA2oxA9* expression, and GA content were grown in glasshouse conditions at 21°C day/18°C night with daylength extended to 16 h by artificial lighting. Four plants were grown in 20-cm pots containing a soil/compost mix supplemented with slow release NPK fertilizer. Plant height was recorded at maturity by measuring the main stem from the surface of the soil to the tip of the spike. The method for determining leaf elongation rates has been previously described (Chandler and Robertson, 1999).

Genetic and Physical Mapping

A F2:F3 mapping population was generated by crossing Icaro with the tall cultivar Langdon. DNA was extracted from the endosperm half of 700 F2 seeds and screened with SNP markers *IWA3230* and *IWB62878* previously shown to flank the *Rht18* locus (Tang, 2015). Twenty recombinants were identified and phenotyped by measuring heights on 4 to 16 F3 progeny from each recombinant in the glasshouse. A Langdon short read cDNA data set (Trick et al., 2012) was downloaded from the Sequence Read Archive, and reads were quality trimmed using Trimmomatic V0.32 (Bolger et al., 2014). Icaro and Langdon reads were mapped with Bowtie2 to the Chinese Spring IWGSC RefSeq v1.0 genome assembly (https://wheat-urgi.versailles.inra.fr/). The mapped reads within the *Rht18* region of interest were visually inspected with the Integrative Genomics Viewer (Robinson et al., 2011) and three SNVs identified and converted to KASP markers (*cs216*, *cs412*, and cs*416*). The 20 recombinants were genotyped, and only one recombination event was identified between *cs216* and *cs416*. The physical location of *GA2oxA9*, the *IWA3230* and *IWB62878* markers from the 90K SNP array, and the *cs216*, *cs412*, and *cs416* markers generated in this study were determined by using their sequences as a query for a BLASTn search of the Chinese Spring IWGSC RefSeq v1.0 genome assembly (https://wheat-urgi.versailles.inra.fr/). Sequences of KASP markers used in this study are shown in Supplemental Table S3.

Mutagenesis and Identification of Overgrowth Mutants

Approximately 4,000 Icaro grains were treated with sodium azide (Chandler and Harding, 2013) and M1 plants grown in an outdoor birdcage area in Canberra in 2013. To evaluate independent mutant events, M2 subpopulations were created by harvesting seed in bulk rows. Approximately 135,000 M2 seeds were sown in plots at the Leeton NSW trial site in 2014. Fourteen overgrowth plants were identified that were 10 to 30 cm taller than Icaro (approximately one overgrowth mutant per 10,000 M2 seed). Five of these lines were selected from different M2 subpopulations and were therefore likely to represent independent events. M3 seed from the 14 overgrowth lines were progeny tested in the glasshouse in 2015 and five overgrowth mutants M12, M17, M22, M24, and M54, which were likely to represent independent events, were selected for further study. M12, M24, and M54 were intercrossed and F2 populations scored for height in the glasshouse. The lack of dwarf lines in the F2 generation indicated that the overgrowth mutations were probably allelic (data not shown). M12 and M24 were also crossed to Icaro and Anhinga. F1 plants from crosses with Icaro were short, indicating that the overgrowth mutation was recessive, and F2 populations segregated for a single dominant dwarfing gene (data not shown). F1 plants from crosses with Anhinga were tall, and the lack of dwarf F2 progeny indicated that the dominant *Rht18* dwarfing effect was lost in these mutants (data not shown).

Overgrowth mutants were also generated in a hexaploid background. Approximately 6,000 grains of the BC_4F_4 Halberd-*Rht18* seed was treated with sodium azide as above and sown in the field in 2014. M2 seed was harvested from three bulked plots and ~300,000 grains were sown in 2015. Screening of the M2 population from one bulked plot identified 110 lines judged to be taller than the bulk population (approximately three overgrowth mutants per 10,000 M2 seed). Eighty of these lines were progeny tested in glasshouse conditions, and 30 have so far been confirmed as overgrowth mutants.

Chromosome Flow Sorting

Suspensions of intact mitotic metaphase chromosomes were prepared from synchronized root tip meristem of young seedlings (Vrána et al., 2000). Prior to flow cytometry, chromosome GAA microsatellite loci were fluorescently labeled using 5′-FITC-GAA7-FITC-3′ and chromosomal DNA was stained by 4′,6-diamidino-2-phenylindole at 2 μg/mL (Vrána et al., 2016). Chromosome samples were analyzed by FASCAria II SORP flow sorter (BD Biosciences). Approximately 35,000 copies of chromosome 6A (equivalent of ~50 ng DNA) were flow sorted from each line into a 0.25-mL PCR tube containing 40 μL of sterile distilled water. Contamination of the sorted 6A fractions by other chromosomes ranged from 3% to 11% (6% average). Chromosomal DNA was then treated with proteinase K, purified, and amplified in three independent reactions (Simková et al., 2008). The amplification products were pooled to reduce amplification bias and at least 7 μg DNA was obtained from each line. To check the chromosome identity and the level of contamination in individual flow-sorted fractions, 2,000 chromosomes were sorted onto a microscopic slide, air-dried, and used for fluorescence in situ hybridization with a probe for GAA microsatellites (Kubaláková et al., 2003).

Chromosome 6A Sequence Analysis

The MutChromSeq protocol was used to identify the new mutations in the overgrowth mutants (Sánchez-Martín et al., 2016). All raw Illumina reads from chromosome 6A DNA of Icaro, Anhinga, and the overgrowth mutants M12, M17, M22, M24, and M54 were quality trimmed using Trimmomatic V0.32 with the default settings for paired end reads (Bolger et al., 2014). The quality trimmed reads from Icaro were de novo assembled using CLC Assembly Cell v 4.3.0 (https://www.qiagenbioinformatics.com/). Assembly quality control was assessed and assembly statistics generated using QUAST (quality assessment tool for genome assemblies; Gurevich et al., 2013). The de novo assembly produced an assembly with a total length of 444 Mb (~70% of the total length of 6A) and an N50 contig length of 1851 bp. The de novo Icaro assembly was masked for highly repetitive repeats regions with RepeatMasker v4.0.6 (http://repeatmasker.org) using the Triticeae Repeat Database (trep-db_complete_Rel-16.fasta) as the external library (http://wheat.pw.usda.gov/ITMI/Repeats/). Quality trimmed reads from Icaro, M12, M17, M22, M24, and M54 were mapped to the de novo Icaro assembly using BWA v0.7.15 (bwa aln) with default settings (Li and Durbin, 2009). SAM files were converted to BAM format (samtools view), duplicates removed (samtools rmdup), and mapped files converted to the mpileup format (samtools mpileup –BQ0) using samtools v1.3.1 (Li et al., 2009). Two custom java scripts Pileup2XML.jar and MutChromSeq.jar (https://github.com/steuernb/MutChromSeq) were used to integrate the Icaro, M12, M17, M22, M24, and M54 mpileup data sets and to identify contigs where all five mutants had an independent SNV (Sánchez-Martín et al., 2016). Potential SNVs were discarded if the allele frequency was less than 99% or total coverage was <10 (Sánchez-Martín et al., 2016).

Comparison of Nucleotide and Amino Acid Sequences

The nucleotide sequences of *GA2oxA9* from Icaro (GenBank accession no. KX163068; Vikhe et al., 2017), M12, M17, M22, M24, and M54 were aligned using MEGA v6.06 (Tamura et al., 2013). Predicted ORFs of *GA2oxA9* from Icaro (Vikhe et al., 2017), M12, M17, M22, M24, and M54 were translated and aligned with the wheat and rice (*Oryza sativa*) GA 2-oxidases, *GA2oxA6*, *GA2oxA9* (Pearce et al., 2015), *OsGA2ox5*, and *OsGA2ox6* (Lo et al., 2008) using MEGA v6.06 (Tamura et al., 2013). The *GA2oxA9* gene was amplified by PCR from genomic DNA from Castelporziano, Capelli, Halberd, Halberd-*Rht18*, and the Halberd overgrowth mutants M1, M10, M13, M26, M30, M46, M47, and

M75. PCR primer sequences are listed in Supplemental Table S4. The products of the PCR reaction were sequenced and the nucleotide, and predicted amino acid sequences were aligned using MEGA v6.06 (Tamura et al., 2013). The sequence 100 kb upstream of the transcriptional start site of *GA2oxA9* from Icaro was compared to Anhinga using the dotmatcher tool (http://www.bioinformatics.nl/cgi-bin/emboss/dotmatcher) with threshold and window size set to 50.

Expression Analysis

For gene expression in peduncles, the basal 25% of elongating peduncles from the main stem were harvested at 50% final length and immediately frozen in liquid nitrogen. For gene expression in the first leaf, the entire leaf was harvested 3 d after germination. RNA was extracted and DNase treated using the MaxwellRSC plant RNA kit (Promega) as per the manufacturer's instructions. First-strand cDNA synthesis primed with oligo dT (18) was performed using Maxima H Minus Reverse Transcriptase (Thermo Scientific) as per the manufacturer's instructions. qPCR was performed using the Bio-Rad384CFX real-time system. qPCR was performed using Platinum Taq DNA polymerase (Life Technologies) and SYBR green. *TaACTIN* was used as the reference gene because its expression was stable across genotypes. Relative transcript levels were calculated using the ΔΔCt method allowing for primer amplification efficiencies as previously described (Deng et al., 2015; Ford et al., 2016). The qPCR primer sequences used in this study are listed in Supplemental Table S4. The products of the *GA2oxA9* and *GA2oxB9* qPCRs were sequenced to confirm their specificity. The qPCR results are the mean values of four biological and two technical replicates, and appropriate no template controls were included and melt curve analysis conducted for all experiments.

GA Content Analysis

For GA content analyses the basal 25% of elongating peduncles including the node from the main stem were harvested at 50% final length and immediately frozen in liquid nitrogen. Each biological replicate consisted of ~2 g fresh weight (FW) of pooled peduncles from at least six individual plants. GA was extracted as previously detailed (Boden et al., 2014). Briefly, tissue was homogenized, covered in 80% methanol overnight, internal standards ($[^2H_2]GA_1$, $[^2H_2]GA_8$, $[^2H_2]GA_{12}$, $[^2H_2]GA_{19}$, $[^2H_2]GA_{20}$, and $[^2H_2]GA_{53}$) were added, and solids were removed by centrifugation. Samples were extracted by passing though C18 Sep-Pak (Waters) followed by SAX column (Maxi-Clean; Grace Davison Discovery Sciences) as previously described. Samples were then derivatized as described (Li et al., 2017a) except that samples were incubated in 200 mM EDC (*N*-(3-dimethylaminopropyl)-*N*′-ethylcarbodiimide hydrochloride; Sigma-Aldrich) in ethanol in 50 μL overnight at 40°C, then dried and resuspended in 30 μL Milli-Q water. Samples were then analyzed using a Waters Acquity H-Class UPLC instrument coupled to a Waters Xevo triple quadrupole mass spectrometer. A Waters Acquity UPLC BEH C_{18} column (2.1 mm × 100 mm × 1.7 μm) was used. The instrument was operated and multiple reaction monitoring (MRM) transitions were monitored (Li et al., 2017a). For all samples, peak areas for endogenous and labeled GAs were compared and combined with FW of sample to calculate ng/g FW.

Functional Assay

The coding sequences of Icaro and M24 were synthesized by Genscript with *Nde*I and *Sal*I restriction sites at the 5′ and 3′ends, respectively. The coding sequence was inserted into pMCSG7 and transformed into BL21 (DE3) cells. Cells were grown overnight at 37°C and used as inoculum for LB cultures containing 200 $\mu g/mL^{-1}$ ampicillin. At an OD_{600} of 0.6 cultures were placed at 23°C and induced with 0.5 mM IPTG overnight. *Escherichia coli* proteins were extracted by French press in extraction buffer according to Macmillan et al. (2005). A GA metabolic assay was performed as previously described (Macmillan et al., 2005). In brief, *E. coli* lysate was incubated with radiolabeled GA precursor in a buffered reaction mixture containing cofactors at 30°C for 1 h before the reaction was stopped with 0.25 volumes of acetic acid. Samples were resuspended in 0.4% acetic acid, and 20 ng of $[^2H_2]GA_{29}$ catabolite was added as an internal standard for metabolite recovery. Samples were loaded onto preconditioned C18 Sep-Pak cartridges and eluted with 100% methanol. Samples were dried and resuspended in 1% acetic acid before running as free acids on a Waters Acquity H-Class UPLC instrument coupled to a Waters Xevo triple quadrupole mass spectrometer. A Waters Acquity UPLC BEH C_{18} column (2.1 mm × 100 mm × 1.7 μm) was used. The instrument was operated as described above. MRM transitions for labeled GA metabolites were determined experimentally from the analysis of standard compounds or analogous $[^2H_2]$ labeled compounds. Samples were compared to various external standards, including genuine $[^2H_2]GA_{110}$, kindly supplied by Prof. Shinjiro Yamaguchi and Dr. Kiyoshi Mashiguchi (Tohoku University, Japan). Peak areas for diagnostic MRM transitions for $[^{14}C_1]GA_{12}$, $[^{14}C_1]GA_{110}$, and $[^2H_2]GA_{29}$ catabolite were recorded, and peak areas for $[^{14}C_1]GA_{12}$ and $[^{14}C_1]GA_{110}$ were adjusted using the $[^2H_2]GA_{29}$ catabolite surrogate standard peak areas.

Statistical Analysis for Plant Height, Expression Analysis, and GA Content

All data presented for plant height, relative expression of *GA2oxA9*, and GA content are mean values ± SE. Differences between mean values of two values were tested by a Student's *t* test assuming a two-tailed distribution and equal variance. Differences between mean values of greater than two genotypes were determined by one-way ANOVA with Tukey's honestly significant difference post-hoc test in the R statistical package.

Accession Numbers

Accession number are as follows: *GA2oxA9*, KX163068;

Supplemental Data

The following supplemental materials are available.

Supplemental Table S1. Comparison of DNA sequence from Icaro and Anhinga 100Kb upstream of the *GA2oxA9* transcription start site.

Supplemental Table S2. Identification of deletions in Icaro compared to Anhinga 5Mb upstream of the *GA2oxA9* transcription start site.

Supplemental Table S3. Sequences of SNP based KASP markers.

Supplemental Table S4. Primer sequences.

Supplemental Figure S1. Nucleotide alignment of *GA2oxA9* from Icaro and overgrowth mutants.

Supplemental Figure S2. Protein alignment of Icaro, overgrowth mutants, and rice and wheat C_{20}-GA 2-oxidases.

Supplemental Figure S3. Nucleotide alignment of *GA2oxA9* from Halberd Isolines.

Supplemental Figure S4. Protein alignment of GA2oxA9 from Hal-*Rht18* and Halberd overgrowth mutants.

Supplemental Figure 5. Leaf elongation rate and *GA2oxA9* expression in rapidly elongating first leaves.

Supplemental Figure S6. Crude and soluble protein extracts from *E. coli* expressing *GA2oxA9* coding sequences of Icaro and M24 separated by SDS_PAGE.

Supplemental Figure 7. The Anhinga and Icaro sequence 100 kb upstream of *GA2oxA9* is highly conserved.

ACKNOWLEDGMENTS

We thank Sergio Gálvez Rojas for assisting with early steps in the bioinformatic analysis and Tanya Phongkham for excellent technical assistance. We also thank Greg Rebetzke for providing Halberd-*Rht18* germplasm and A/Prof. John Ross from University of Tasmania and Philippa Borrill from the John Innes Centre for critical discussions and suggestions. We thank Zdeňka Dubská and Romana Šperková for technical assistance with chromosome sorting. We thank Brande Wulff for providing access to CLC license and computing facilities at John Innes Centre. Carl Davies has contributed photographic skills and generated the graphics.

Received January 11, 2018; accepted March 4, 2018; published March 15, 2018.

LITERATURE CITED

Appleford NE, Wilkinson MD, Ma Q, Evans DJ, Stone MC, Pearce SP, Powers SJ, Thomas SG, Jones HD, Phillips AL, Hedden P, Lenton JR

(2007) Decreased shoot stature and grain α-amylase activity following ectopic expression of a gibberellin 2-oxidase gene in transgenic wheat. J Exp Bot **58:** 3213–3226

Boden SA, Weiss D, Ross JJ, Davies NW, Trevaskis B, Chandler PM, Swain SM (2014) EARLY FLOWERING 3 regulates flowering in spring barley by mediating gibberellin production and FLOWERING LOCUS T expression. Plant Cell **26:** 1557–1569

Bolger AM, Lohse M, Usadel B (2014) Trimmomatic: a flexible trimmer for Illumina sequence data. Bioinformatics **30:** 2114–2120

Borrill P, Adamski N, Uauy C (2015) Genomics as the key to unlocking the polyploid potential of wheat. New Phytol **208:** 1008–1022

Busov VB, Meilan R, Pearce DW, Ma C, Rood SB, Strauss SH (2003) Activation tagging of a dominant gibberellin catabolism gene (*GA 2-oxidase*) from poplar that regulates tree stature. Plant Physiol **132:** 1283–1291

Chandler PM, Robertson M (1999) Gibberellin dose-response curves and the characterization of dwarf mutants of barley. Plant Physiol **120:** 623–632

Chandler PM, Harding CA (2013) 'Overgrowth' mutants in barley and wheat: new alleles and phenotypes of the 'Green Revolution' *DELLA* gene. J Exp Bot **64:** 1603–1613

Deng WW, Clausen J, Boden S, Oliver SN, Casao MC, Ford B, Anderssen RS, Trevaskis B (2015) Dawn and dusk set states of the circadian oscillator in sprouting Barley (*Hordeum vulgare*) seedlings. PLoS One **10:** e0129781

Elias AA, Busov VB, Kosola KR, Ma C, Etherington E, Shevchenko O, Gandhi H, Pearce DW, Rood SB, Strauss SH (2012) Green revolution trees: semidwarfism transgenes modify gibberellins, promote root growth, enhance morphological diversity, and reduce competitiveness in hybrid poplar. Plant Physiol **160:** 1130–1144

Ellis MH, Rebetzke GJ, Chandler P, Bonnett D, Spielmeyer W, Richards RA (2004) The effect of different height reducing genes on the early growth of wheat. Funct Plant Biol **31:** 583–589

Ford B, Deng W, Clausen J, Oliver S, Boden S, Hemming M, Trevaskis B (2016) Barley (*Hordeum vulgare*) circadian clock genes can respond rapidly to temperature in an EARLY FLOWERING 3-dependent manner. J Exp Bot **67:** 5517–5528

Gale MD, Youssefian S, Russell GE (1985) Dwarfing genes in wheat. *In* GE Russell, ed, Progress in Plant Breeding 1. Butterworth-Heinemann, London, pp 1–35

Giorgi D, Farina A, Grosso V, Gennaro A, Ceoloni C, Lucretti S (2013) FISHIS: fluorescence in situ hybridization in suspension and chromosome flow sorting made easy. PLoS One **8:** e57994

Gurevich A, Saveliev V, Vyahhi N, Tesler G (2013) QUAST: quality assessment tool for genome assemblies. Bioinformatics **29:** 1072–1075

Haque MA, Martinek P, Watanabe N, Kuboyama T (2011) Genetic mapping of gibberellic acid-sensitive genes for semi-dwarfism in durum wheat. Cereal Res Commun **39:** 171–178

Hedden P (2003) The genes of the Green Revolution. Trends Genet **19:** 5–9

Hedden P, Thomas SG (2012) Gibberellin biosynthesis and its regulation. Biochem J **444:** 11–25

Huang J, Tang D, Shen Y, Qin B, Hong L, You A, Li M, Wang X, Yu H, Gu M, Cheng Z (2010) Activation of gibberellin 2-oxidase 6 decreases active gibberellin levels and creates a dominant semi-dwarf phenotype in rice (*Oryza sativa* L.). J Genet Genomics **37:** 23–36

Jia Q, Li C, Shang Y, Zhu J, Hua W, Wang J, Yang J, Zhang G (2015) Molecular characterization and functional analysis of barley semi-dwarf mutant Riso no. 9265. BMC Genomics **16:** 927

Konzak CF (1988) Evaluation and genetic analysis of semi-dwarf mutants of wheat. *In* Semi-Dwarf Cereal Mutants and Their Use in Cross-Breeding: Research Coordination Meeting 1981. International Atomic Energy Agency, Vienna, Austria, pp 25–37

Koornneef M, Dellaert LWM, van der Veen JH (1982) EMS- and radiation-induced mutation frequencies at individual loci in *Arabidopsis thaliana* (L.) Heynh. Mutat Res **93:** 109–123

Kubaláková M, Valárik M, Barto J, Vrána J, Číhalíková J, Molnár-Láng M, Dolezel J (2003) Analysis and sorting of rye (*Secale cereale* L.) chromosomes using flow cytometry. Genome **46:** 893–905

Li D, Guo Z, Liu C, Li J, Xu W, Chen Y (2017a) Quantification of near-attomole gibberellins in floral organs dissected from a single *Arabidopsis thaliana* flower. Plant J **91:** 547–557

Li H, Durbin R (2009) Fast and accurate short read alignment with Burrows-Wheeler transform. Bioinformatics **25:** 1754–1760

Li H, Handsaker B, Wysoker A, Fennell T, Ruan J, Homer N, Marth G, Abecasis G, Durbin R; 1000 Genome Project Data Processing Subgroup (2009) The Sequence Alignment/Map format and SAMtools. Bioinformatics **25:** 2078–2079

Li H, Torres-Garcia J, Latrasse D, Benhamed M, Schilderink S, Zhou W, Kulikova O, Hirt H, Bisseling T (2017b) Plant-specific histone deacetylases HDT1/2 regulate *GIBBERELLIN 2-OXIDASE 2* expression to control Arabidopsis root meristem cell number. Plant Cell **29:** 2183–2196

Lo SF, Yang SY, Chen KT, Hsing YI, Zeevaart JA, Chen LJ, Yu SM (2008) A novel class of gibberellin 2-oxidases control semidwarfism, tillering, and root development in rice. Plant Cell **20:** 2603–2618

Lo SF, Ho TD, Liu YL, Jiang MJ, Hsieh KT, Chen KT, Yu LC, Lee MH, Chen CY, Huang TP, et al (2017) Ectopic expression of specific GA2 oxidase mutants promotes yield and stress tolerance in rice. Plant Biotechnol J **15:** 850–864

Macmillan CP, Blundell CA, King RW (2005) Flowering of the grass *Lolium perenne*: effects of vernalization and long days on gibberellin biosynthesis and signaling. Plant Physiol **138:** 1794–1806

Pearce S, Huttly AK, Prosser IM, Li YD, Vaughan SP, Gallova B, Patil A, Coghill JA, Dubcovsky J, Hedden P, Phillips AL (2015) Heterologous expression and transcript analysis of gibberellin biosynthetic genes of grasses reveals novel functionality in the *GA3ox* family. BMC Plant Biol **15:** 130

Peng J, Richards DE, Hartley NM, Murphy GP, Devos KM, Flintham JE, Beales J, Fish LJ, Worland AJ, Pelica F, et al (1999) 'Green revolution' genes encode mutant gibberellin response modulators. Nature **400:** 256–261

Robinson JT, Thorvaldsdóttir H, Winckler W, Guttman M, Lander ES, Getz G, Mesirov JP (2011) Integrative genomics viewer. Nat Biotechnol **29:** 24–26

Sakai M, Sakamoto T, Saito T, Matsuoka M, Tanaka H, Kobayashi M (2003) Expression of novel rice gibberellin 2-oxidase gene is under homeostatic regulation by biologically active gibberellins. J Plant Res **116:** 161–164

Sakamoto T, Kobayashi M, Itoh H, Tagiri A, Kayano T, Tanaka H, Iwahori S, Matsuoka M (2001) Expression of a gibberellin 2-oxidase gene around the shoot apex is related to phase transition in rice. Plant Physiol **125:** 1508–1516

Sakamoto T, Morinaka Y, Ishiyama K, Kobayashi M, Itoh H, Kayano T, Iwahori S, Matsuoka M, Tanaka H (2003) Genetic manipulation of gibberellin metabolism in transgenic rice. Nat Biotechnol **21:** 909–913

Sánchez-Martín J, Steuernagel B, Ghosh S, Herren G, Hurni S, Adamski N, Vrána J, Kubaláková M, Krattinger SG, Wicker T, et al (2016) Rapid gene isolation in barley and wheat by mutant chromosome sequencing. Genome Biol **17:** 221

Sasaki A, Ashikari M, Ueguchi-Tanaka M, Itoh H, Nishimura A, Swapan D, Ishiyama K, Saito T, Kobayashi M, Khush GS, Kitano H, Matsuoka M (2002) Green revolution: a mutant gibberellin-synthesis gene in rice. Nature **416:** 701–702

Schomburg FM, Bizzell CM, Lee DJ, Zeevaart JA, Amasino RM (2003) Overexpression of a novel class of gibberellin 2-oxidases decreases gibberellin levels and creates dwarf plants. Plant Cell **15:** 151–163

Simková H, Svensson JT, Condamine P, Hribová E, Suchánková P, Bhat PR, Bartos J, Safár J, Close TJ, Dolezel J (2008) Coupling amplified DNA from flow-sorted chromosomes to high-density SNP mapping in barley. BMC Genomics **9:** 294

Spielmeyer W, Ellis MH, Chandler PM (2002) Semidwarf (*sd-1*), "green revolution" rice, contains a defective gibberellin 20-oxidase gene. Proc Natl Acad Sci USA **99:** 9043–9048

Spray CR, Kobayashi M, Suzuki Y, Phinney BO, Gaskin P, MacMillan J (1996) The *dwarf-1* (*d1*) mutant of *Zea mays* blocks three steps in the gibberellin-biosynthetic pathway. Proc Natl Acad Sci USA **93:** 10515–10518

Tamura K, Stecher G, Peterson D, Filipski A, Kumar S (2013) MEGA6: Molecular Evolutionary Genetics Analysis version 6.0. Mol Biol Evol **30:** 2725–2729

Tang T (2015) Physiological and genetic studies of an alternative semi-dwarfing gene *Rht18* in wheat. PhD dissertation. University of Tasmania, Australia

Trick M, Adamski NM, Mugford SG, Jiang CC, Febrer M, Uauy C (2012) Combining SNP discovery from next-generation sequencing data with bulked segregant analysis (BSA) to fine-map genes in polyploid wheat. BMC Plant Biol **12:** 14

Vikhe P, Patil R, Chavan A, Oak M, Tamhankar S (2017) Mapping gibberellin-sensitive dwarfing locus *Rht18* in durum wheat and development of SSR and SNP markers for selection in breeding. Mol Breed **37:** 28

Vrána J, Kubaláková M, Simková H, Číhalíková J, Lysák MA, Dolezel J (2000) Flow sorting of mitotic chromosomes in common wheat (*Triticum aestivum* L.). Genetics **156:** 2033–2041

Vrána J, Cápal P, Číhalíková J, Kubaláková M, Doležel J (2016) Flow sorting plant chromosomes – *In* SF Kianian, PMA Kianian, eds, Plant Cytogenetics: Methods and Protocols. Springer, New York, pp 119–134

Wuddineh WA, Mazarei M, Zhang J, Poovaiah CR, Mann DG, Ziebell A, Sykes RW, Davis MF, Udvardi MK, Stewart CN Jr (2015) Identification and overexpression of *gibberellin 2-oxidase* (*GA2ox*) in switchgrass (*Panicum virgatum* L.) for improved plant architecture and reduced biomass recalcitrance. Plant Biotechnol J **13:** 636–647

Würschum T, Langer SM, Longin CFH, Tucker MR, Leiser WL (2017) A modern Green Revolution gene for reduced height in wheat. Plant J **92:** 892–903

Yamaguchi S (2008) Gibberellin metabolism and its regulation. Annu Rev Plant Biol **59:** 225–251

Yang ZY, Zheng JC, Liu CY, Wang YS, Condon AG, Chen YF, Hu YG (2015) Effects of the GA-responsive dwarfing gene *Rht18* from tetraploid wheat on agronomic traits of common wheat. Field Crops Res **183:** 92–101

Zimin AV, Puiu D, Hall R, Kingan S, Clavijo BJ, Salzberg SL (2017) The first near-complete assembly of the hexaploid bread wheat genome, *Triticum aestivum.* Gigascience **6:** 1–7